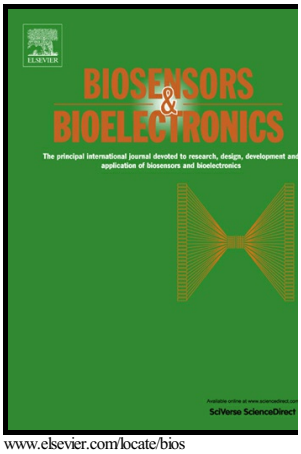

A sensitive photoelectrochemical biosensor for AFP detection based on ZnO inverse opal electrodes with signal amplification of CdS-QDs

Ru Xu, Yandong Jiang, Lei Xia, Tianxiang Zhang, Lin Xu, Shuang Zhang, Dali Liu, Hongwei Song

www.elsevier.com/locate/bios

PII: S0956-5663(15)30204-9
DOI: http://dx.doi.org/10.1016/j.bios.2015.06.037
Reference: BIOS7773

To appear in: *Biosensors and Bioelectronic*

Received date: 18 March 2015
Revised date: 15 June 2015
Accepted date: 17 June 2015

Cite this article as: Ru Xu, Yandong Jiang, Lei Xia, Tianxiang Zhang, Lin Xu Shuang Zhang, Dali Liu and Hongwei Song, A sensitive photoelectrochemica biosensor for AFP detection based on ZnO inverse opal electrodes with signa amplification of CdS-QDs, *Biosensors and Bioelectronic* http://dx.doi.org/10.1016/j.bios.2015.06.037

A sensitive photoelectrochemical biosensor for AFP detection based on ZnO inverse opal electrodes with signal amplification of CdS-QDs

Ru Xu†, Yandong Jiang†, Lei Xia†, Tianxiang Zhang†, Lin Xu†, Shuang Zhang†, Dali Liu*†, Hongwei Song*†‡

†State Key Laboratory on Integrated Optoelectronics, College of Electronic Science and Engineering, Jilin University, 2699 Qianjin Street, Changchun, 130012, P. R. China.

‡The State Key Laboratory of Bioelectronics, Southeast University, 210096 P. R. China.

Corresponding to:

Prof. Dali Liu E-Mail: ldl@jlu.edu.cn Tel: 86-431-85168241

Prof. Hongwei Song E-Mail: songhw@jlu.edu.cn Tel: 86-431-81736614

Abstract

In this work, ZnO inverse opals structure (IOs) based photoelectrochemical (PEC) electrode was fabricated for alpha-fetoprotein (AFP) detection. Then, the uniform CdS quantum dots (QDs) were hydrothermally synthesized, which allowed the binding of AFP and glucose oxidase (GOD) on CdS QDs, forming the AFP-CdS-GOD composite. The competitive immunosensor of AFP and the AFP-CdS-GOD composite with anti-AFP antibodies (Ab) immobilized on FTO (fluorine-doped tin oxide) /ZnO IOs electrode was successfully applied to the detection of AFP. GOD could catalyze glucose to produce hydrogen peroxide (H_2O_2) acting as an electron donor to scavenge photogenerated holes in the valence band of CdS QDs, reducing the recombination of electrons and holes of CdS QDs. Also the effective energy level matching between the conduction bands of CdS QDs and ZnO widened the range of light absorption, allowing for electron injection from excited CdS QDs to ZnO upon visible light irradiation, which enhanced the photocurrent. The results show that the immunosensor of AFP possesses a large linear detection range of 0.1 - 500 ng/ml with a detection limit of 0.01 ng/ml. It also exhibits excellent anti-interference property and acceptable stability. This work provides a promising method for achieving excellent photoelectrochemical biosensor detection of other proteins.

Keywords: ZnO inverse opals structure, CdS QDs, AFP detection, photoelectrochemical biosensor

1. Introduction

AFP, a major plasma protein, mainly generates from the liver, yolk sac and fetal human gastrointestinal tract (Tomasi, 1977). High concentrations of AFP found in adult serum is very possible a symptom of malignant tumor, which can be taken as a specific diagnosis of primary liver cancer clinical indicators. Thus sensitive and accurate early detection and diagnosis is of crucial importance (Srinivas et al., 2001). So far, many techniques have been developed for the detection of AFP, such as enzyme-linked immunoassay (ELISA) (Liew et al., 2007), electrochemical luminescence (ECL) (Qian et al., 2010; Yang et al., 2009), electrochemical method (Dai et al., 2011; Tang et al., 2010; Zhang et al., 2011), mass spectrometry (Stevens et al., 2008), quartz crystal microbalance (QCM) (Chou et al., 2002) and surface plasmon resonance (SPR) (Teramura and Iwata, 2007) immunity determination. Although good sensitivity has been achieved, these protocols were labor-intensive, time-consuming and not suitable for rapid analysis. So it is still very necessary to develop a novel, highly sensitive and alternative detection method of AFP. As a widely attracted for the interest of method, PEC measurements have successfully detected numerous materials, such as glucose, ascorbic acid, cysteine, AFP and carcinoembryonic antigen (Li et al., 2013; Li et al., 2012; Xia et al., 2014; Zhao et al., 2012; Wen and Ju, 2015). In addition, PEC biosensors are detection methods based on photocatalytic oxidation or reduction biological molecules, which make photogenerated electrons transferred between the semiconductor electrode and the substances to be detected under light to enhance the PEC response (Wang et al., 2009).

Combining the advantages of both fluorescence sensing and electrochemical sensing, the complete separation of excitation source (light) and detection signal (current) could greatly reduce the undesired background signal (Liang et al., 2006). Photosensitive material, as the principal part of PEC sensing, is critical to the performance of the sensor. Although PEC biosensor has been widely used to detect biological molecules, few photosensitive materials can be available for it (Kang et al., 2010).

As is known, ZnO is an n-type wide-band-gap semiconductor material with a bandwidth of about 3.37 eV, which makes it a good candidate for photoelectronic applications (Arya et al., 2012). Many ZnO nanostructures, including nanorods (Hu et al., 2010), nanotubes (Dai et al., 2009), nanowires (Wan et al., 2004), nanosheets (Tsai et al., 2014), nanoclusters(Zhao et al., 2007), hollow nanospheres (Fang et al., 2011) and nanoflowers (Zhang et al., 2014a) have been applied in biosensor. IO structure is a kind of three-dimensional photonic crystal (3D-PC). The slow light effect in 3D-PC could increase the effective optical path length and increase the photovoltaic response on photovoltaic cells and the photochemical process (Sakoda, 1999; Baba, 2008; Chen et al., 2006, 2007, 2008). Additionally, the uniform porous structures of inverse opals photonic crystal(IOPCs) possess a large surface area which is helpful of electron transfer and biomolecule immobilization, and shorten the distance of electron diffusion between the FTO substrate and the immobilized subatance, thereby facilitating the capability of electron transfer (Xia et al., 2014).

ZnO has been widely applied in photocatalysis, because of its chemical stability, non-toxicity, biocompatibility and powerful electronic communications (Zhang et al., 2004; Zhu et al., 2007). However, the wide-band-gap of ZnO allows it to absorb only the ultraviolet light (<380 nm), limiting the sufficient utilization of solar light. Besides, UV light's strong oxidizing ability may destroy biological molecules (Li et al., 2012; Tak et al., 2008). The critical challenge for ZnO electrode is the efficient utilization of the visible light. Accordingly, one strategy is the usage of narrow-band-gap QDs, including CdS, CdSe, CdTe, and PbS (Robel et al., 2006; Peter et al., 2002; Robert Plass et al., 2002; Zhang et al., 2014), which can generate multiple electron–hole pairs per photon to improve the efficiency of utilizing visible light(Shen et al., 2011).

On the basis of the above ideas, we synthesized the ZnO IOs-CdS QDs composites and applied them to the PEC sensing. Scheme 1 indicates how the FTO/ZnO IOs electrode were modified and the basic principle of PEC detection. First, chitosan (CS) was modified on FTO/ZnO IOs electrode. CS as a biocompatible material with high permeability was fixed on FTO/ZnO IOs electrode for further immobilization of Anti-AFP antibody (Ab). Then, AFP and GOD were connected on CdS QDs to form the AFP-CdS-GOD composite, which were used to improve the sensitivity of immunsensor by the competitive reaction of AFP and AFP-CdS-GOD with the Ab immobilized on FTO/ZnO electrode. The effective level matching of CdS QDs and ZnO would make fully use of visible light and suppress the damage of UV to proteins. The test was carried out in 60 mM glucose solution. GOD can catalyze glucose to generate H_2O_2 as electron donor, which supplements electrons for CdS

valence band, thereby further increasing photocurrent and improving the detection sensitivity.

(A)

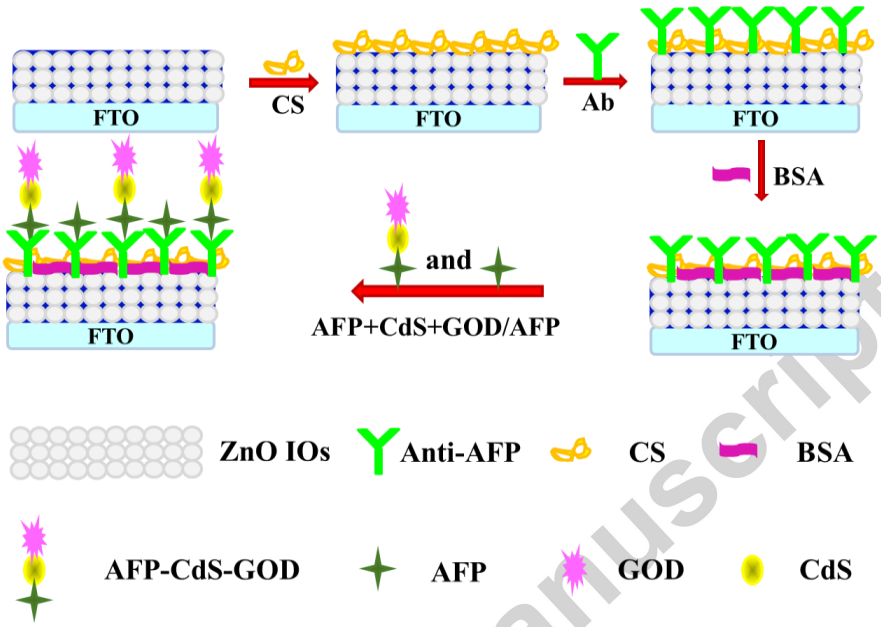

(B)

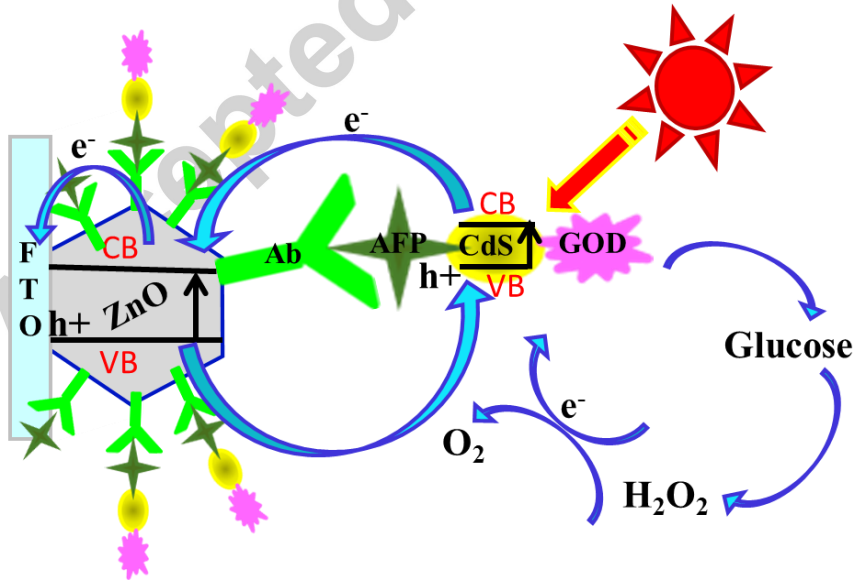

Scheme1. Preparation processes and principles of the immunosensor.

2. Results and discussion

2.1. Characterizations of the FTO/ZnO IOs Electrode.

ZnO IOs were prepared by the sol - gel method using the polymethylmethacrylate (PMMA) latex sphere colloidal as colloidal crystals templates (See in Supplementary information). ZnO nanometer materials possess the properties of biocompatibility and stability that make them become an environmentally friendly semiconductor material applied to PEC sensor. Meanwhile, IOs structure is very suitable for producing sensor due to large surface area, chemical, physical and electronic communication properties. In Fig.1A, the field emission scanning electron microscope (SEM) image of ZnO IOs shows an orderly arrangement rule of pore structure in a 3D space, with pore size of about 270 nm. Fig.1B shows the SEM image of ZnO IOs modified by CS on its framework. As it shown clearly, CS is adhered to the surface of ZnO IOs. The orderly macroporous structure of ZnO IOs greatly widens its surface area so that more CS could adhere to its surface and interior. Fig.1C shows the X-ray diffractometry (XRD) patterns of ZnO IOs powder. It presents good hexagonal matching (JCPDS, card number 36-1451). No peaks of impurity are observed, indicating that the sample is pure ZnO of hexagonal phase. Fig.1D presents the Fourier-transform infrared (FTIR) absorption spectra of ZnO IOs, CS and ZnO/CS, respectively. As to CS, the absorption peak around 3400 cm^{-1} is caused by the overlapping of hydrogen bond association -OH stretching vibration mode and -NH stretching vibration mode and their broadening(Menon et al., 2011). The two stretching vibration peaks of C-H are at 2860 cm^{-1} and 2925 cm^{-1},and the absorption peaks of Amide Ⅰ and Amide Ⅱ are at about 1625 cm^{-1} and 1428

cm^{-1}, respectively. The typical absorption peaks of amide I and amide II also exist in the sample of ZnO/CS, which indicate that the surface of ZnO IOs adhered by CS maintained its basic characteristics, thus revealing the good biological compatibility of ZnO IOs.

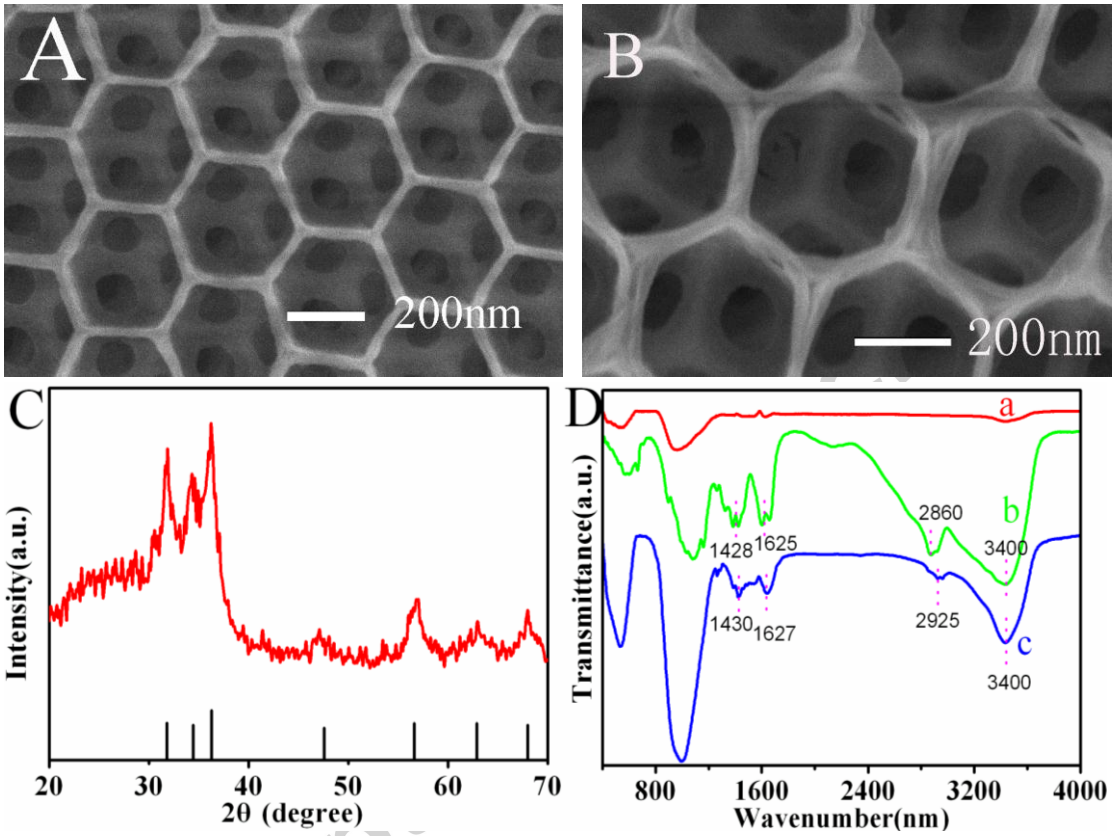

Fig.1. SEM image: ZnO IOs (A), ZnO IOs modified to CS (B), XRD pattern of ZnO IOs powder (C), FTIR absorption spectrum (D): (a) ZnO IOs powder (red line), (b) CS powder (green line), (c) ZnO IOs modified by CS (blue line).

2.2. Characterization of AFP-CdS-GOD.

CdS QDs was synthesized using a modified version of the hydrothermal method (Li et al., 2007, see in Supplementary materials). The UV-VIS absorption spectra were used to characterize CdS QDs (Fig.S1). As shown in Fig.2, the UV- VIS absorption spectra prove the successful interconnection between CdS QDs, GOD and AFP. Fig.2

exhibits the absorption spectra of CdS QDs, GOD, AFP, AFP-CdS, CdS-GOD and the AFP-CdS-GOD composite. The absorption peak of CdS QDs appears at about 500nm, which can effectively widen the absorbent scopes. The character peaks of AFP and GOD appear at 280nm, corresponding to π-π * transitions in the tryptophan and tyrosine residues of the proteins. Comparing with the above absorption spectra, the absorption peak of 500nm and 280nm are simultaneously discovered in AFP-CdS, CdS-GOD and AFP-CdS-GOD, which are mainly caused by AFP and GOD. This suggests that AFP and GOD are successfully connected to CdS QDs.

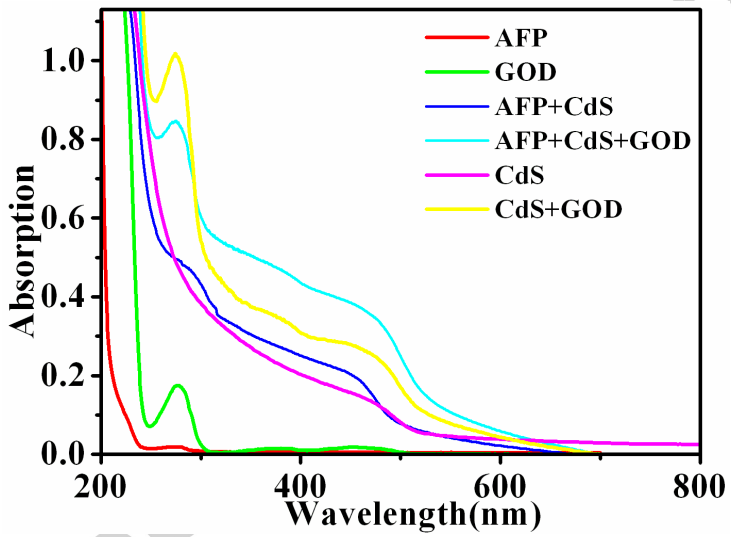

Fig.2. UV - visible absorption spectrum of CdS QDs, AFP, GOD, AFP-CdS, CdS-GOD and AFP-CdS-GOD composites.

2.3. Effect of experimental conditions on photocurrent response.

The applied potential is an important factor for photocurrent. Fig.S2A shows that the photocurrent increases from -0.3~0.8 V, which indicates that the photogenerated electrons are effectively driven to the counter electrode by the positive potential that is beneficial to charge separation. Therefore, 0.6 V was selected as the applied potential

in this work. Four electrodes were prepared with photonic stop band (PSB) positions at 588 nm, 600 nm, 628 nm and 628 nm and named as S1-588, S2-600, S3-628 and S4-628, respectively. The inset picture of Fig.S2B shows the transmission spectra of the four samples, indicating the good structure of IOs sample. The ZnO IOs electrodes were used to detect AFP (100 ng/ mL). Fig.S2B displays the photocurrent of AFP detection to ZnO IOs electrodes with different PSB positions and depth. For the IOs with different PSB positions and band gap depth, the photocurrents are 1.49 μA, 1.22 μA, 1.55 μA and 1.32 μA, respectively. The variations of PSB positions and depth lead no regular change to the phototcurrent, which indicate that the PSB positions and depth lead of IOs have no obvious effect on the photocurrent. This could be attributed to shallow PSB for the IOs. The pH value of the detection solution was also investigated in the amperometric response. The pH can influence the activity of Ab, AFP, as well as GOD immobilized on the surface of electrode. Fig.S2C shows the variations of the photocurrent at FTO/ZnO-AFP-CdS-GOD with the detection solution of different pH. Considering the stability of the supporting skeleton of ZnO and the activity of Ab, AFP and GOD, the photocurrent was detected in the pH range 5.8–8.0. Obviously, the optimal current was obtained at pH=7.4. Therefore, detection solution with a pH of 7.4 was used in further experiments.

2.4. Characterizing the fabrication process of photoelectrochemical biosensor.

As is known, electrochemical impedance spectroscopy (EIS) is an effective and

convenient method for probing the each reaction step of the modified electrode. Each reaction step of the modified electrode was analyzed by EIS in the frequency range 0.01 to 100 kHz, and in a KCl (0.1 M) solution containing a redox probe of 5 mM $K_3[Fe(CN)_6]$-$K_4[Fe(CN)_6]$ (1 : 1) mixture at an open-circuit potential of 20 mV. Fig.S2D represents the Nyquist diagrams of each electrode involving different construction step of the PEC biosensor. The electron transfer resistance (R_{et}) is equal to the diameter of the semicircle. First, the probe was presented to the surface of FTO /ZnO IOs electrode, obtaining a value of R_{et}. Subsequently, CS was modified on the surface of FTO/ZnO IOs electrode, resulting in the increase of R_{et}. Then, Ab, BSA and the AFP-CdS-GOD composite were constructed step by step, and the R_{et} of each related electrode increased correspondingly, which indicate that the added substance hindered the access of the electronic transmission to the electrode surface. Therefore, all the growth of R_{et} prove that the successful connection of all substances to the electrode. The optimum R_{et} was obtained when the AFP-CdS-GOD composite was fixed on the PEC biosensor, which was due to GOD hindering the electronic transmission. The elevating hindrance effect and insulating effect introduced by biological materials suggest successful stepwise fabrication of the biosensor.

The fabrication of immunosensor also can be proved by monitoring the change of photocurrent, as shown in Fig.3A. The bared FTO electrode shows nearly zero photocurrent. After the surface of FTO was modified with ZnO IOs, the photocurrent increased obviously. Photocurrent declines gradually after immobilization of CS, Ab and BSA on electrode. These can be explained that the immobilization of these

organics hinder electronic transmission. The photocurrent enhances slightly when the AFP-CdS was connected to the electrode, because the connection of CdS QDs on the electrode through specific antibody-antigen immunoreactions can broaden the absorbent range of light. That led to separation of photogenerated electron-hole pairs followed by fast electron injection from the excited CdS QDs to the conduction band of ZnO. However, the photocurrent still increases as the AFP-CdS-GOD composite were also immobilized on the developed immunosensor through specific antibody-antigen immunoreactions. It can be explained by the fact that GOD catalyzes glucose into H_2O_2, which can generate more electrons in the process of decomposition. This would deplete the photogenerated holes located at the valence band of excited CdS and facilitate the charge separation, thus further increasing the photocurrent. The inset of Fig. 3B presents cyclic voltammograms (CVs) in 5 mM $K_3[Fe(CN)_6]$ solution, with the purpose to track the prepared ZnO IOs surfaced. When the FTO/ZnO IOs electrode was modified by CS (curve b), as compared with FTO/ZnO IOs electrode (curve a) a decreased current response signal was obtained. This is because the successful immobilization of CS on the surface FTO/ZnO IOs electrode which could form an electron-blocking layer and hinder the efficiency electron transfer. Then, sequentially further decreased current were observed after the loading of Ab (curve c) and BSA (curve d). CVs indicate the successful fabrication process of the electrode. Fig. 3B displays CVs of the FTO/ZnO-AFP-CdS-GOD immunosensor in the absence (green) and in the presence of 60 mM of glucose (red) in contact with a 0.1 M PBS (pH=7.4) solution. In this case, GOD catalyzes glucose to gluconolactone, while the

electrons involved in the process are immediately transferred to the valence band of CdS QDs which leads to the increase of the peak current.

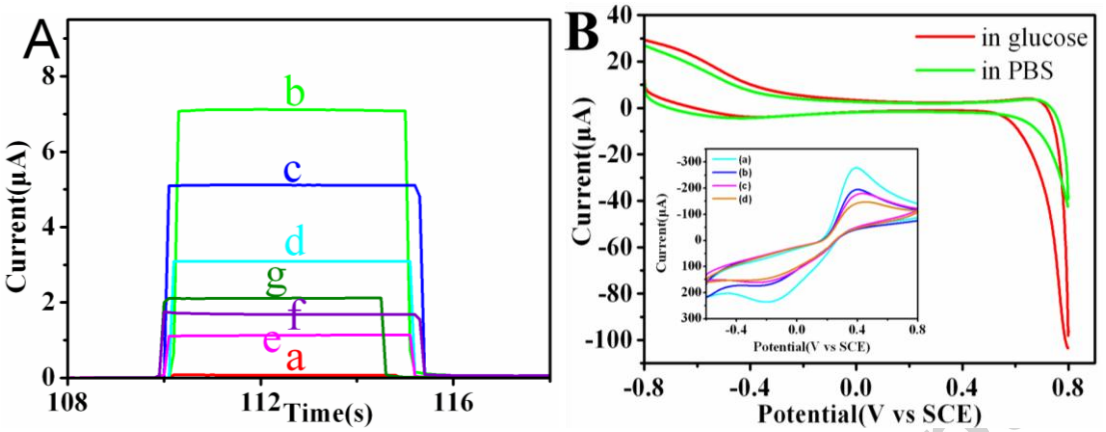

Fig.3.. (A) Photocurrent of modified each substance: (a) FTO, (b) FTO/ZnO, (c) FTO/ZnO/CS, (d) FTO/ZnO/CS/Ab, (e) FTO/ZnO/CS/Ab/BSA and (f) FTO/ZnO/CS/Ab/BSA connection 25 μL AFP-CdS (10 μL) and AFP (15 μL, 100 ng/ml) mixed solution and (g) FTO/ZnO/CS/Ab/BSA connection 25 μL AFP-CdS-GOD (10 μL) and AFP (15 μL, 100 ng/ml) mixed solution, (B) CVs of the FTO/ZNO-AFP-CdS-GOD immunosensor in 0.1M PBS(pH=7.4, green) and presence of 60 mM glucose (red), respectively. (Inset) CVs of the fabrication progress of (a) FTO/ZnO, (b) FTO/ZnO/CS, (c) FTO/ZnO/CS/Ab, (d) FTO/ZnO/CS/Ab/BSA in 5 mM $K_3[Fe(CN)_6]$ solution.

2.5. Photoelectrochemical detection of AFP.

AFP detection is based on the immune competitive interaction of Ab with AFP and the AFP-CdS-GOD composite. The AFP (15 μL) of a certain concentration and the AFP-CdS-GOD composite (10 μL) were mixed together, and then the mixture were immobilized on the electrode after blocking with BSA. As a result, a novel competitive immune sensor works. Fig.4A shows the PEC intensity for detecting the different concentrations of AFP at an applied potential of 0.6 V with a 500 W xenon lamp irradiation, whereas Fig.4B shows derived calibration curves of the

developed immunosensor used for the determination of the concentration of AFP in PBS (0.01 M, pH=7.2) and human serum. The photocurrent–time curve clearly illustrates the rapid response of the modified electrode to different concentrations of AFP. Since the concentration of AFP to be detected is much lower than the AFP-CdS-GOD composite, more AFP are immobilized on the biosensor with the AFP increasing concentrations, leading to decreased photocurrent intensity. The photocurrent decrement was proportional to the logarithmic value of AFP concentration, ranging from 0.1 ng/ml to 500 ng/ml with a correlation coefficient of 0.9886. The regression equation was $\Delta I=2.8796-0.5982 \lg (C_{AFP}$ ng/ml), with a detection limit of 0.01 ng/ml (S/N=3). Fig.4C shows the stability of the photocurrent response of the PEC sensor. The photocurrent responses were recorded as the excitation light was turned on and off for 10 times. No great changes were distinguished in photocurrent, which indicates that this PEC sensor has quite acceptable stability. Furthermore, the optical signal can turn stable in only 5 seconds, implying the shorter response time of detection. Besides, the long-term stability of this immunosensor was also examined by storing the immunosensor in a refrigerator at 4 ^{o}C. After 9 days of storage, the added AFP concentration of Sample 1, Sample 2 changed by 47% and 140%, respectively, indicating an acceptable long-term stability (Table S1). The reproducibility of the electrode is assessed by an interassay of relative standard deviation (RSD). By assaying the same 100ng/mL AFP samples with five electrodes, RSD of 5.4% is obtained, indicating satisfactory reproducibility (Fig.S3). Table 1 shows the results obtained from the proposed biosensor were consistent with

other biosensor. The result shows enough sensitivity for the detection of AFP.

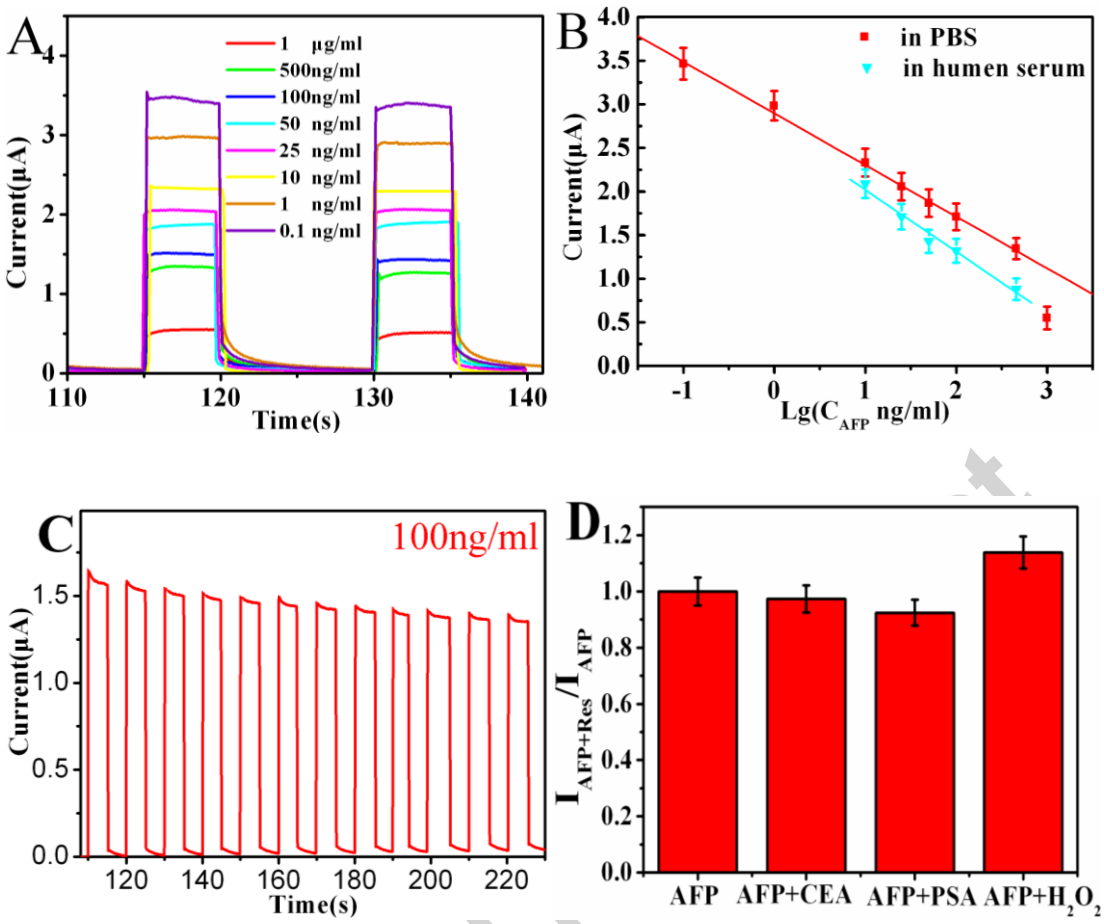

Fig.4. (A) photocurrent response, (B) the corresponding calibration curve of different concentrations of AFP in PBS (red) and in human serum.(blue), (C) the stabilization of PEC signal, repeatability test of turning on /turning off electrodes once every 5S in the PBS solution (0.1 M, pH = 7.4) containg 60 mM glucose. (D) The selectivity of the immunoassay by comparing to the interfering proteins: containing AFP-CdS-GOD and 100 ng / mL of AFP alone or with 500 ng/ml CEA, 500 ng/ml PSA and 0.1 mM H_2O_2. Error bars show the standard deviation of repeated measurements.

Table 1 Comparison of several immunosensors of AFP detection.

Electrode	Detection range (ng/ml)	LOD	Ref.
ZnO	0.1 ~ 500 ng/ml	0.01 ng/ml	This work
TiO2	0.05 ~ 50 ng/mL	0.04 ng/ml	Wang et al.,
CuO	0.05 ~ 500 ng/mL	0.038 ng/ml	Wen et al., 2015

2.6. Specificity of the immunosensor

One of the concerns about an immunosensor is the resistance to interference from irrelevant contaminants. The specificity of the sensor are investigated by connecting the AFP-CdS-GOD composite to electrodes with 100 ng/ml of AFP without or with 500 ng/ml of carcinoembryonic antigen (CEA) , 500 ng/ml of prostate specific antigen (PSA) and 1mM of H_2O_2 respectively. Results seen in Fig.4D, the single interfering protein at five-fold concentration of AFP have no obvious influence on the PEC response of AFP. Compared with the photocurrent caused by AFP alone, the variation in current caused by H_2O_2 is about 10%. The results indicate that the observed photoelectric current is mainly produced by specific binding, and can make sure that photoelectric chemical sensors have a good specificity

3. Conclusions.

In conclusion, the sensitive PEC immunosensor based on the FTO /ZnO IOs electrode with signal amplification of CdS-QDs have been prepared successfully. ZnO IOs perform the crucial role of the antibody immobilized. Besides, the AFP-CdS-GOD composites are immobilized on the developed immunosensor through specific antibody-antigen immunoreactions, with CdS QDs broadening the absorption

to visible light and GOD catalyzing glucose, providing electrons and strengthening photocurrent. The results show that the PEC immunoassay achieved has high sensitivity to AFP, and the linear ranges of 0.1-500 ng/ml with a low detection limit (LOD) of 0.01 ng/ml, meeting the detect requirement. The immunosensor has excellent reproducibility, acceptable long time stability and good specificity. The present design of the immune sensor may be of crucial significance to the clinical and biological analysis of protein.

Acknowledgments

This work was supported by the Major State Basic Research Development Program of China (973 Program, 2014CB643506), the National Natural Science Foundation of China (Grant no. 11374127, 61204015, and 81301289), the Jilin Province Natural Science Foundation of China (No. 20140101171JC), the Open Research Fund of State Key Laboratory of Bioelectronics, Southeast University and Program for Chang Jiang Scholars and Innovative Research Team in University (IRT13018), and Graduate Innovation Fund of Jilin University (project 2014094).

References

Arya, S.K., Saha, S., Ramirez-Vick, J.E., Gupta, V., Bhansali, S., Singh, S.P., 2012. Anal. Chim. Acta 737, 1-21

Baba, T., 2008. Nat. Photonics 2, 465–473.

Chen, J.I.L., Freymann, G., von, Choi, S.Y., Kitaev, V., Ozin, G.A., 2006. Adv. Mater. 18 (14), 1915–1919.

Chen, J.I.L., Freymann, G., von, Kitaev, V., Ozin, G.A., 2007. J. Am. Chem. Soc. 129 (5), 1196–1202.

Chen, J.I.L., Loso, E., Ebrahim, N., Ozin, G.A., 2008. J. Am. Chem. Soc. 130 (16), 5420–5421.

Chou, S.F., Hsu, W.L., Hwang, J.M., Chen, C.Y., 2002. Clin. Chem. 48 (6), 913-918.

Dai, Y.X., Cai, Y.Y., Zhao, Y.F., Wu, D., Liu, B., Li, R., Yang, M.H., Wei, Q., Du, B., Li, H., 2011. Biosens. Bioelectron. 28 (1), 112-116.

Dai, Z., Shao, G., Hong, J., Bao, J., Shen, J., 2009. Biosens. Bioelectron. 24 (5), 1286-1291.

Fang, B., Zhang, C., Wang, G., Wang, M., Ji, Y., 2011. Sen. Actu. B-Chem. 155 (1), 304-310.

Hu, W., Liu, Y., Zhu, Z., Yang, H., Li, C.M., 2010. ACS Appl. Mater. Inter. 2 (6), 1569-1572.

Robel, I., Subramanian, V., Kuno, M., Kamat, P.V., 2006. J. Am. Chem. Soc. 128, 46556-45674.

Kang, Q., Yang, L. X., Chen, Y. F., Luo, S. L., Wen, L. F., Cai, Q. Y., Yao, S. Z., 2010. Anal. Chem. 82 (23), 9749-9754.

Li, H., Shih, W. Y., Shih, W. H., 2007. Ind. Eng. Chem. Res. 46 (7), 2013-2019.

Li, H.X., Hao, W.L., Hu, J.C., Wu, H.Y., 2013. Biosens. Bioelectron. 47, 225-230.

Li, Y. J., Ma, M. J., Zhu, J. J., 2012. Anal. Chem. 84 (23), 10492-10499.

Liang, M.M., Liu, S.L., Wei, M.Y., Guo, L.H., 2006. Anal. Chem. 78 (2), 621-623.

Liew. M., Groll, M.C., Thompson, J.E., Call, S.L., Moser, J.E., Hoopes, J.D., Voelkerdingl, K., Wittwer, C., Spendlove, R.S., 2007. Biotechniques 42 (3), 327-333.

Menon, D., Thomas, R.T., Narayanan, S., Maya, S., Jayakumar, R., Hussain, F., Lakshmanan, V.K., Nair, S.V., 2011. Carbohyd. Polym. 84 (3), 887-893.

Peter, L,M., Riley, D,J., Tull, E,J., Wijayantha. K.G.U., 2002. Chem. Commun. 10, 1030-1031.

Qian, J., Zhou, Z,X., Cao, X,D., Liu, S,Q., 2010. Anal. Chim. Acta. 665 (1), 32-38.

Plass, R., Pelet, S., Krueger, J., Gra1tzel, M., 2002. J. Phys. Chem. B 106, 7578-7580.

Sakoda, K., 1999. Opt. Express 4 (5), 167–176.

Shen, Q., Zhao, X., Zhou, S., Hou, W., Zhu, J.J., 2011. J. Phys. Chem. C 115 (36), 17958-17964.

Srinivas, P. R., Kramer, B. S., Srivastava, S., 2001. Lancet Oncol. 2 (11), 698-704.

Stevens, S.M., Prokai-Tatrai, K., Prokai, L., 2008. Mol. Cell. Proteomics 7 (12), 2442-2451.

Tak, Y., Kim, H., Lee, D., Yong, K., 2008. Chem. Commun. 38, 4585-4587.

Tang, J.A., Su, B.L., Tang, D.P., Chen, G.N., 2010. Biosens. Bioelectron. 25(12), 2657-2662.

Teramura, Y., Iwata, H., 2007. Anal. Biochem. 365 (2), 201-207.

Tomasi, T. B., Jr., 1977. Annu. Rev. Med. 28, 453-465.

Tsai, F.S., Wang, S.J., 2014. Sens. Actu. B-Chem 193, 280-287

Wan, Q., Li, Q.H., Chen, Y.J., Wang, T.H., He, X.L., Gao, X.G., Li, J.P., 2004. Appl. Phys. Lett. 84 (16), 3085.

Wang, G.L., Yu, P.P., Xu, J.J., Chen, H.Y., 2009. J. Phys. Chem. C 113 (25), 11142-11148.

Wen, G.M., Ju, H.X., 2015. Talanta 134, 496-500.

Xia, L., Song, J., Xu, R., Liu, D.L., Dong, B., Xu, L., Song, H.W., 2014. Biosens. Bioelectron. 59, 350-357.

Yang, X.Y., Guo, Y.S., Bi, S., Zhang, S.S., 2009. Biosens. Bioelectron. 24(8), 2707-2711.

Zhang, B., Tang, D.P., Liu, B.Q., Chen, H.F., Cui, Y.L., Chen, G.N., 2011. Biosens. Bioelectron. 28(1), 174-180.

Zhang, B., Lu, L., Hu, Q., Huang, F., Lin, Z., 2014a. Biosens. Bioelectron. 56, 243-249.

Zhang, C., Wang, L., Wang, A., Zhang, S., Mao, C., Song, J., Niu, H., Jin, B., Tian, Y., 2014. Appl. Sur. Sci. 315, 22-27.

Zhang, F., Wang, X., Ai, S., Sun, Z., Wan, Q., Zhu, Z., Xian, Y., Jin, L., Yamamoto, K., 2004. Anal. Chim. Acta. 519 (2), 155-160.

Zhao, W.W., Ma, Z.Y., Yan, D.Y., Xu, J.J., Chen, H.Y., 2012. Anal. Chem. 84 (24), 10518-10521.

Zhao, Z.W., Chen, X.J., Tay, B.K., Chen, J.S., Han, Z.J., Khor, K.A., 2007. Biosens. Bioelectron. 23 (1), 135-139.

Zhu, X., Yuri, I., Gan, X., Suzuki, I., Li, G., 2007. Biosens. Bioelectron. 22 (8), 1600-1604.

Zhu, Y.S., Xu, W., Zhang, H.Z., Wang, W., Xu, S., Song, H.W., 2012. J. Phys. Chem. C 116 (3), 2297–2302.

Highlights

1. The sensitive photoelectrochemical immunosensor based on the composites of ZnO IOs with signal amplification of CdS-QDs have been prepared successfully on a disposable FTO substrate.

2. The detection of AFP possesses largely linear detection range of 0.1-500 ng/mL with a detection limit of 0.01 ng / mL.